

Supplementary Data

Preparation of $\text{Mn}_2\text{O}_3/\text{MIL-100}(\text{Fe})$ composite and its mechanism for enhancing the photocatalytic removal of Rhodamine B in water under visible light and persulfate activation

Nguyen Trung Dung^{1,*}, Tran Thi Hue¹, Vu Dinh Thao¹, Nguyen Nhat Huy^{2,3,*}

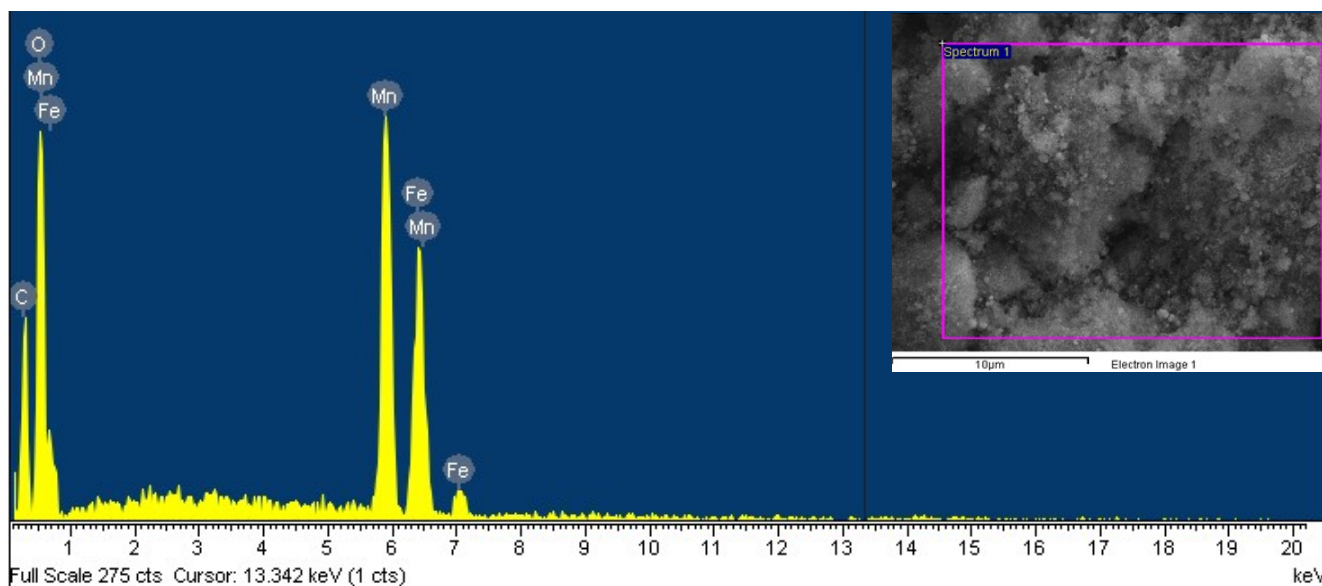


Figure S1. EDX spectrum of M100Mn(60:40)

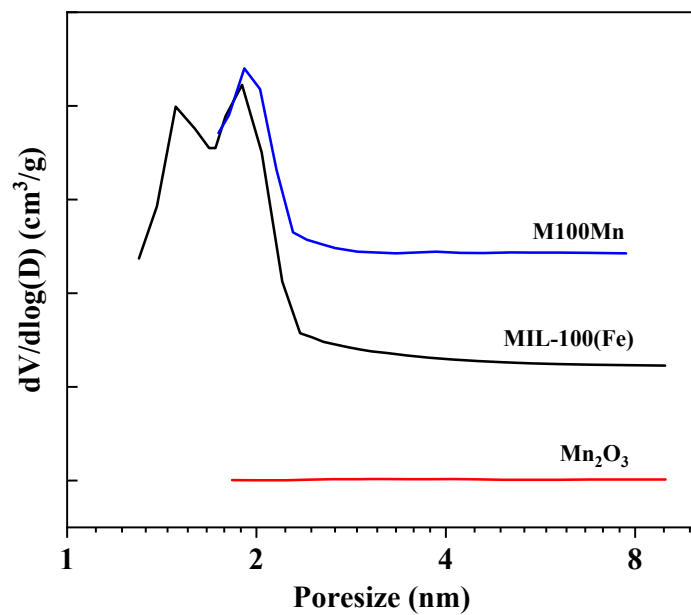


Figure S2. Pore size distribution of Mn₂O₃, MIL-100(Fe), and M100Mn(60:40) materials

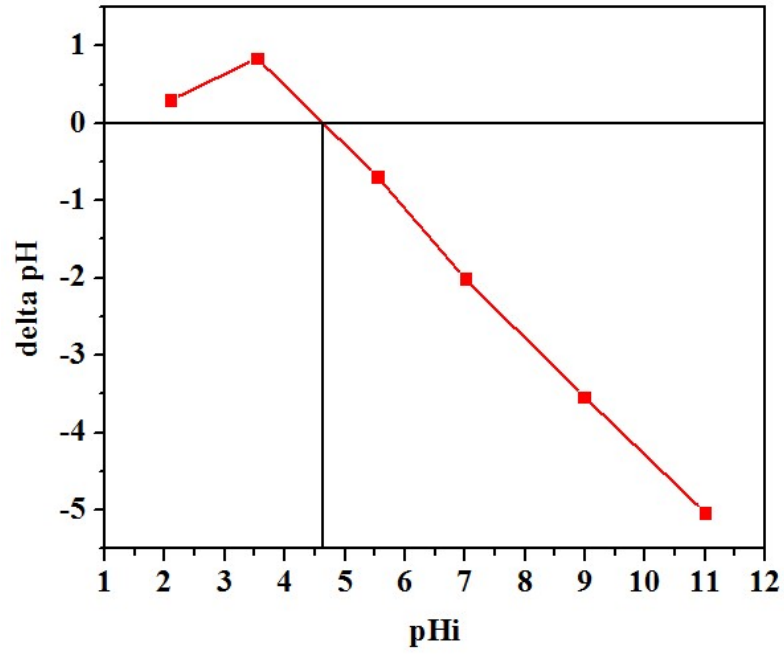


Figure S3. Plot for determining the pH_{pzc} of the M100Mn(60:40) material

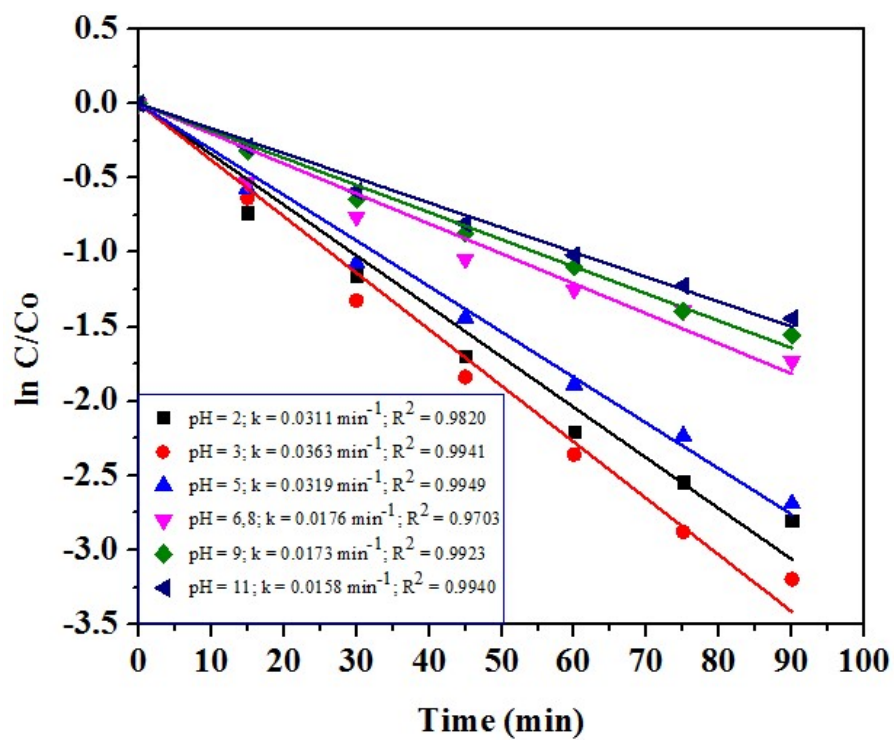


Figure S4. Degradation rate constant of RhB by the M100Mn/Na₂S₂O₈/Vis system with different solution pH

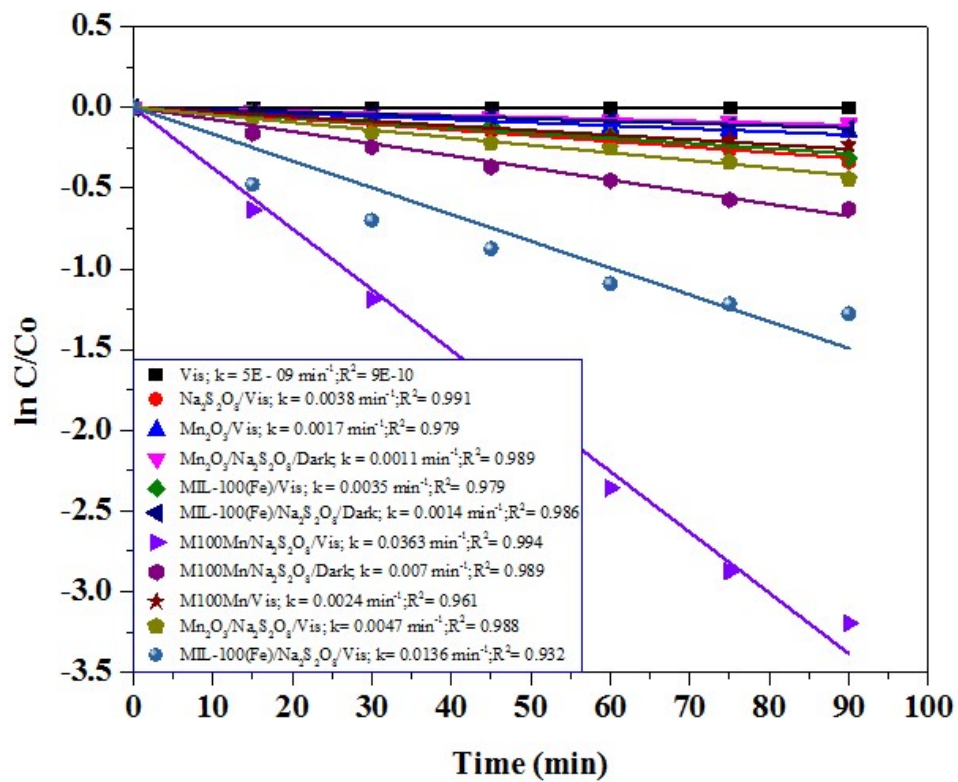


Figure S5. Degradation rate constant of RhB in different reaction systems

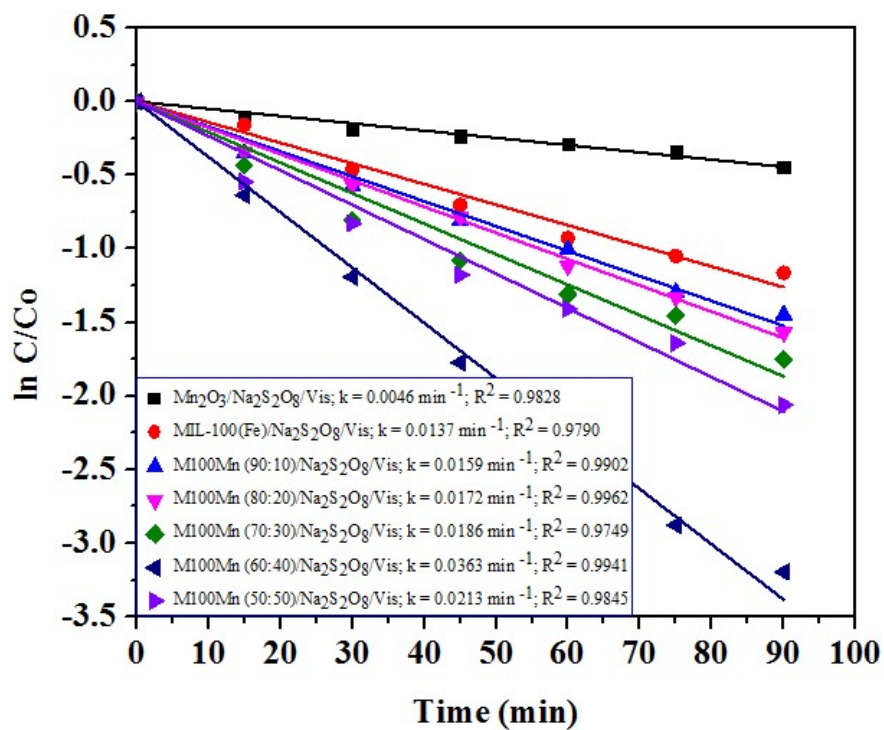


Figure S6. Degradation rate constant of RhB by M100Mn composites with different MIL-100(Fe): Mn_2O_3 ratios

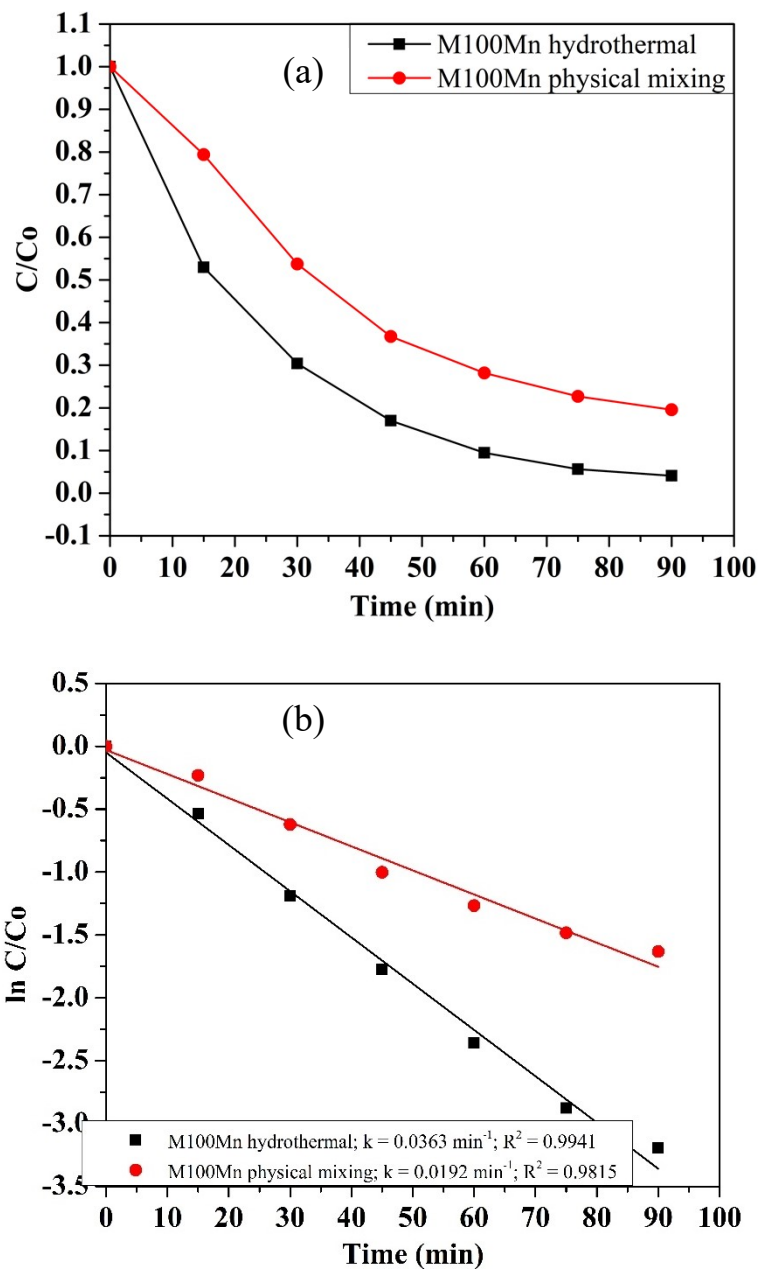


Figure S7. RhB degradation efficiency (a) and rate constant (b) using M100Mn(60:40) with hydrothermal synthesis and physical mixing methods.

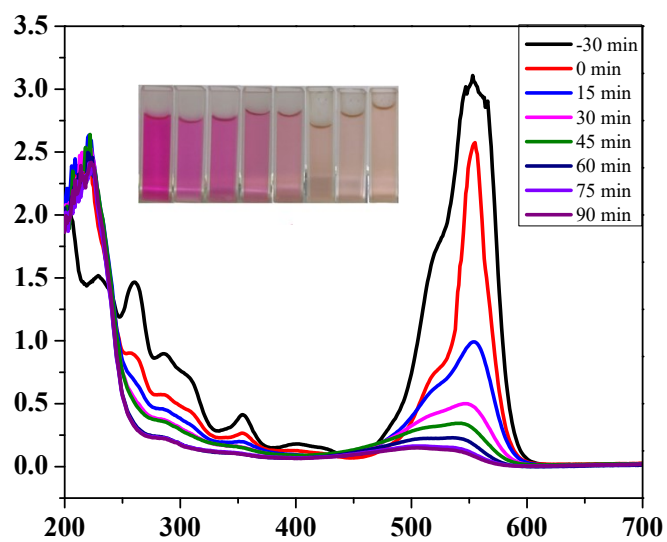


Figure S8. UV-Vis spectra of RhB solution during 30 min of adsorption and 90 min of photocatalytic reaction using M100Mn(60:40)

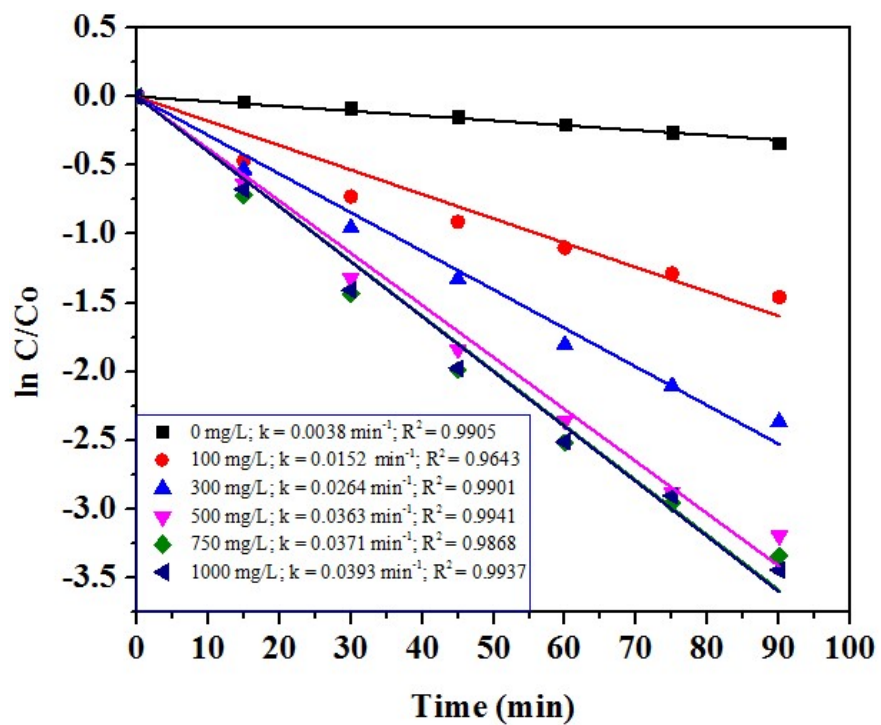


Figure S9. Degradation rate constant of RhB at different M100Mn(60:40) dosages

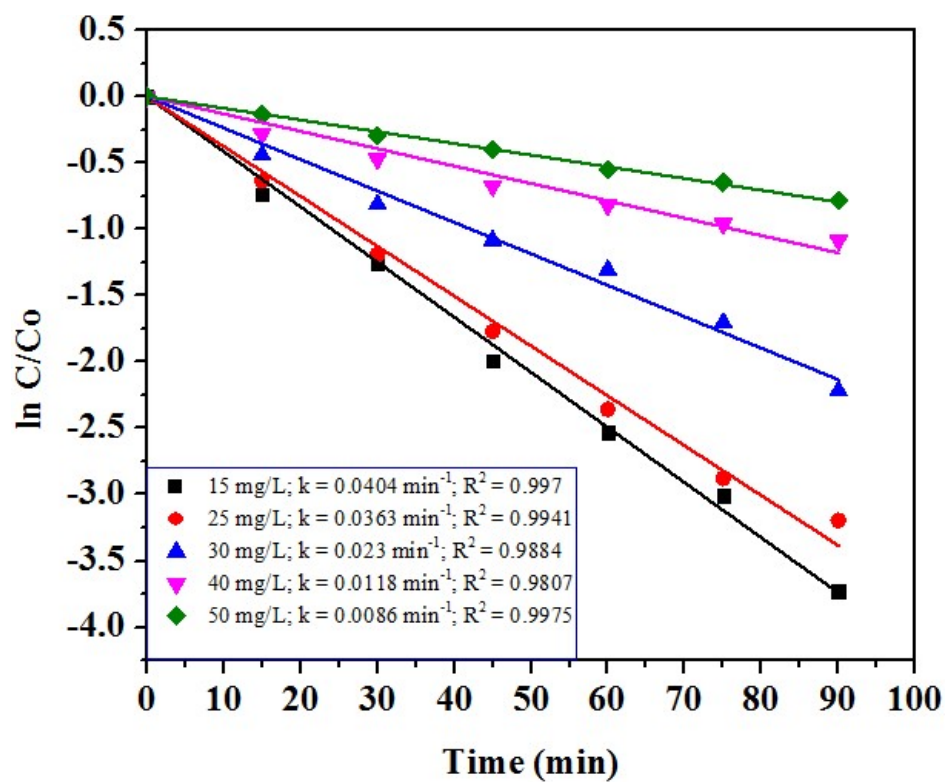


Figure S10. Degradation rate constant of RhB at different initial RhB concentrations

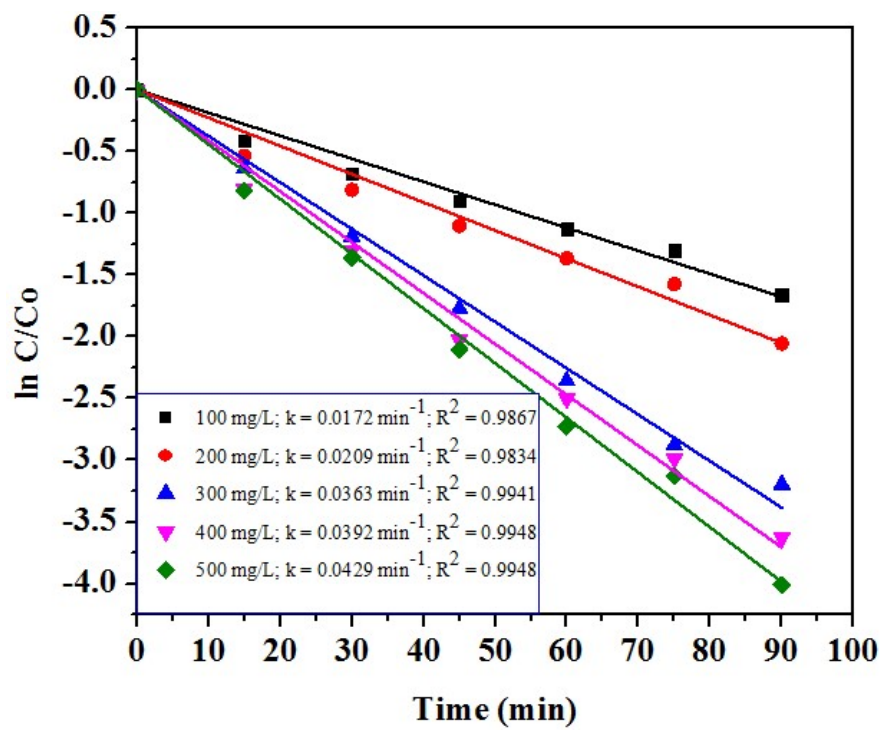


Figure S11. Degradation rate constant of RhB at different Na₂S₂O₈ concentrations

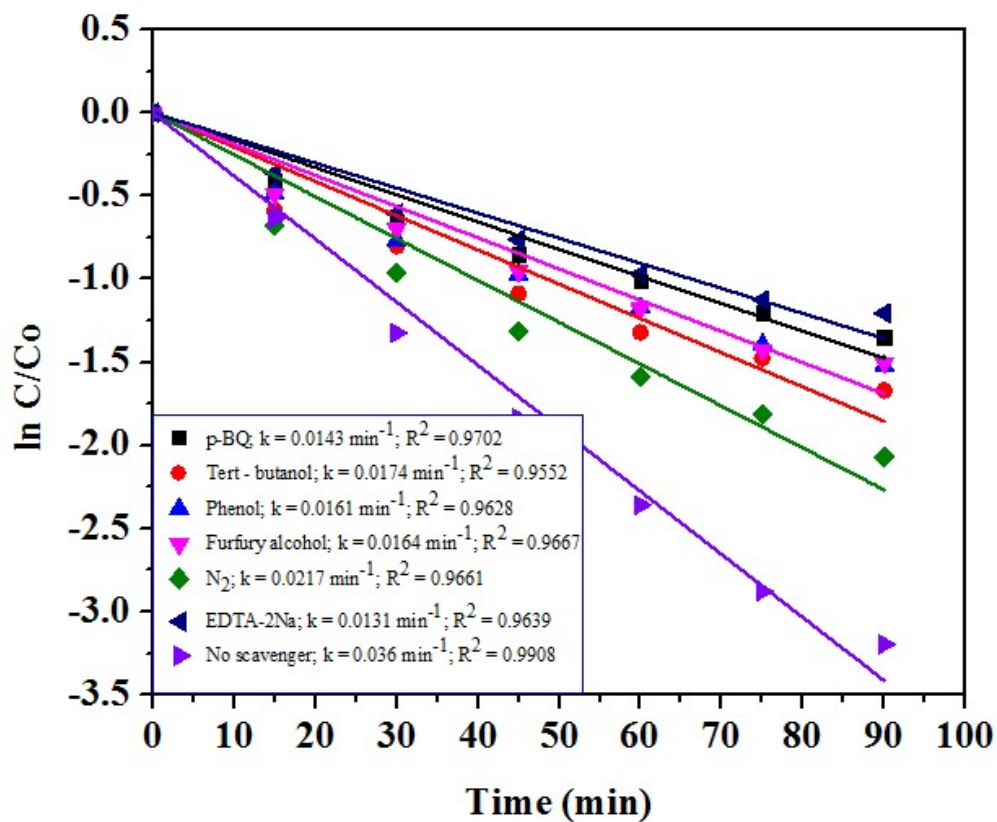


Figure S12. Degradation rate constant of RhB under the presence of different radical scavengers